Institut für Aerodynamik u. Gasdynamik
der Universität Stuttgart (TH)

THE INCOMPRESSIBLE FLUID MOTION DOWNSTREAM OF TWODIMENSIONAL TOLLMIEN SCHLICHTING WAVES

by
Franz Xaver Wortmann
Institut für Aerodynamik und Gasdynamik
Universität Stuttgart
Pfaffenwaldring 21, 7000 Stuttgart 80
Germany

77-5

SUMMARY

In a water tunnel detailed flow field measurements are made of the "natural" deformation of two-dimensional Tollmien waves. The waves are stimulated by a vibrating ribbon and amplified over to ten to thirteen wave lengths. The spanwise position of the breakdown was not fixed by any roughness in the test section. The results suppose for the incipient transition a three-dimensional structure composed by the basic flow and longitudinal counterrotating sheets of vorticity which are inclined downstream and overlap each other like roof shingles.

1. INTRODUCTION

The phenomena which transform the two-dimensional boundary layer waves into a three-dimensional pattern are in contrast to the breakdown process very rarely investigated and not well understood. So far only the work of Klebanoff and his group at the NBS /1/ has dealt with the incipient stages of the transition.

The difficulties of such a task are manifold. The primary requirements are a tunnel with an extreme high signal to noise ratio and an instrumentation which has at least partly a synoptic capability and a high resolution in space and time. This paper concentrates on the structure of the three-dimensional wave, where the spanwise component is still small relative to the streamwise component of the basic two-dimensional wave.

2. EQUIPMENT AND PROCEDURE

The following tests were done in a water tunnel with a test section of 20 x 80 cm cross area and a length of 500 cm. It is described in /2/. The laminar boundary layers at the glass side walls and the top wall are stabilized by suction. Top and bottom walls are slightly curved with a radius of 20 m. The ratio δ^*/R is near $6 \cdot 10^{-4}$. Only the boundary layer on the convex bottom is investigated. The measurements were done mostly with the hydrogene bubble technique and a hot film probe in combination with a plotter. The coordinates are used in the conventional manner with x = flow direction, y = wall distance, z = spanwise position.

All main test conditions as temperatur (18,7°C), tunnel speed (9.93 cm/s at $x_1 = 40$), suction intensity and the geometry of the tunnel walls and the ribbon amplitude were held fixed with extreme care over several months.

The two-dimensional waves were excited in the conventional manner by an oscillating ribbon, 200 cm downstream of the entrance of the test section. Its cross section is 3 x 0.04 mm, the wall distance 0.8 mm, the amplitude ± 0.05 mm. The ribbon has a uniform motion over 72 cm, i.e. 90 % of the tunnel span. The frequency in all measurements was 1/5.49 sec, yielding a wave length of 18.5 cm.

The main test region begins at x_T = 355 cm downstream of the entrance and has a 5 cm grid on the bottom. The numbers on the grid denote the distance $x_1 = x_T - x_T$ in centimeters from the 355 cm station. At x_1 = 40 cm the boundary layer thicknesses are δ = 36.5 mm, δ^* = 12.9 mm, ϑ = 4.46 mm and re_{δ^*} = 1230.

It was our intention to work as much as possible with "natural" conditions and not to enforce certain types of perturbation. For this reason the ribbon is placed far upstream of the test region and used with extreme low amplitudes. In order to get large amplitudes in the test region without increasing the tunnel speed we decided to adjust the top of the tunnel slightly divergent. The associated pressure gradient is practically linear in the test region with a gradient $\Delta U_\infty/U_\infty$ (x_1 = 40) = -5.2 %.

The observed amplification rates are given in Table I. Downstream of x_1 = 30 the amplification at z = - 3 cm is less than at z = - 11 cm, the center line of the three-dimensional development. No roughness or any other artificial means were used to induce a three-dimensional perturbation. Therefore, a large amplitude u'/U_∞ of the Tollmien-Schlichting-wave of about 4 % is necessary in order to become receptive to the faint residual perturbation inherent to the tunnel. This happens at $x_1 \approx 40$, roughly ten to eleven wave lengths downstream of the ribbon. The total amplification from the ribbon to the test region is of the order 3000.

3. OBSERVATIONS AND MEASUREMENTS

Fig.1 gives a perspective view of some ink streaklines in the test section shortly before breakdown. The white plastic sheet on the back side of the transparent bottom, which makes the dark streaklines visible, can be removed. Then a black background allows the

observation of the small hydrogene bubbles seen in the following pictures.

Fig.2 shows the actual spanwise development of the breakdown process for x_1 -positions between x_1 = 55 cm and x_1 = 65 cm. The quadratic grid scale is 5 cm. There are two spanwise locations (z = -11 cm and z = +18 cm) where two "heads" evolve from the time lines. The z = -11 cm position was selected for further investigation. Fig.3 gives an impression of three gross features in this region: the formation of helical vorticity concentration, first observed by Kovasznay et al. /3/ and the fast spread of this configuration in spanwise direction. A little further downstream the top vortex loop conceived by Theodorsen /4/ and first observed by Hama /5/ can be seen. The small pearls on the bubble wire have an average distance of 1 cm.

When these "heads" arise the trailing vortex tubes between two such heads merge each other and roll up also into a tail vortex loop (the counterpart of the top loop) which is seen in Fig.4. All these phenomena are characterized by extremely high velocity gradients in space and time. Therefore we decided to leave these more dramatic events to a later investigation and to begin with the more gradual events associated with the incipient transition where the two-dimensional wave transforms into the three-dimensional wave, roughly one wavelength upstream of Fig.2 and 3.

It can clearly be stated that the three-dimensional event can be a local single event and periodicity is not a necessary condition. Therefore in the following only the motion around the centerline near z = -11 cm is investigated.

The method of measurement is illustrated in Fig.5. The pulsed wire yields the u(z)-profile for a certain wall distance and phase position. The small interruptions indicate the w-component. The time between the front bubble line and the wire is nearly 1/10 of the wave period. The photographs are taken with a tele-photolens (250 mm) in a distance of around 1,6 m in order to reduce the perspective angle and the influence of the v-component.

The evaluation of such measurements over one wave period and four different wall distances are given in Fig.6. The loops indicate the way along which the tip of the velocity vector turns around and describes a sort of Lissajous figure. The sense of circulation with increasing time is to the left on the right side of the plane of symmetry (z = -11 cm) and vice versa for the other side. With other words, when the wave reduces the flow velocity the spanwise w-components point in general to the center line.

One would like to have data with less scatter, smaller amplitudes and better symmetry. A few explanations may be appropriate: the information of Fig.6 can not be gathered in a single wave, in fact we have taken 4 x 12 = 48 different waves and a lot of time. Additionally the spanwise perturbation was not fixed by a roughness element, which may explain some of the scatter. Other sources which cause a certain lack of symmetry and the nonlinear behaviour of the w-component, will be discussed a little later.

The most salient feature of Fig.6 is the orientation of the longitudinal axis of the loops which changes continuously for different wall distances, indicating a continuous shift in the relative phase position of the w-component. In the upper part of Fig.7 the w-component at z = -8 cm is replotted as a function of time or phase position and exhibits the nonharmonic character and the phase shift more clearly. In the lower part of Fig.7 the values of w are again evaluated to yield a piece of the w(y,t) distribution. The latter can be easier and more directly attributed to the ω_x-vorticity component. With the help of a 45° mirror it is possible to look upstream on to a boundary layer profile and to observe the w-component as a distorsion of the boundary layer profile.

Fig.8 shows such a photograph for the z-station z = -7 cm which compares well with the crossplotted results of Fig.7. It is interesting that Klebanoff /1/ had investigated obviously the same phenomenon and got in his Fig.14 and 15 the same result without coming to the same conclusions.

4. DISCUSSION

If we try to interpret the findings of Fig.6 - 8, we have to remember some of the kinematic relationships between velocity and vorticity in the boundary layer: Assuming a local warping of the velocity profile u(z) at constant height the field of vortex tubes acquires components in x- and y-direction. If we consider only the additional ω_x and ω_y components we find that this part of the vorticity field is inclined in downstream direction with a maximum where the slope of the vortex tube has its maximum. When the warping of the velocity profile changes sign only the sense of rotation of the longitudinal vorticity changes but the inclination remains the same.

Now in Fig.6 at the phase position 7 and y = 13 mm we have an u(z)-profile with a slight excess and for phase 3 a more pronounced deficit. According to the foregoing there exist besides the basic ω_z-field two downstream inclined sheets of counterrotating longitudinal vorticity which follow each other with a distance of half a wave length. This holds with opposite signs of rotation for both sides of the x-ẏ-plane of symmetry. The nodal points of Fig.7 and 8 are interpreted as the center of these inclined vorticity sheets and their downward movement with time at a fixed observation point indicates the slope of the sheets in flow direction. These vorticity sheets overlap each other like roof shingles. Fig.9 sketches this model.

Clearly in Fig.6 - 8 we have already a developed state of this shingle model, where the one vortex sheet associated with the velocity deficit has gained much more strength than the other one. Klebanoff /1/ has interpreted his one or two point measurement only in the sense that a longitudinal vortex is mainly in the convex part of the wave and that this rules out the Görtler-Witting instability.

Let us stress the shingle-model a little more: it is not too difficult to imagine a less developed state, where the three-dimensional amplitude is much weaker and of the same size in the front and rear halves of a Tollmien-Schlichting wave. Now, if we assume for the two-dimensional wave a finite amplitude, the prospects of the two longitudinal vorticity sheets are quite different. First: due to the basic wave both sheets are separated from each other not only streamwise but also with respect to the wall distance. Second: the two-dimensional wave has modulated the basic vorticity field and yields two regions where the ω_z-vorticity concentrates to a local maximum. Both regions are wave-bound and situated in the convex and concave part of the wave. The first one is high up, around $y \approx 2\delta^*$ and the other one is down at the wall. The latter one has no freedom to warp, neither vertically nor horizontally. It is fixed by the outer wave and the wall and stays straight in spanwise direction. As a local vorticity maximum it will slave the neighbourhood. If, as in our roof-shingle model, the vortex tubes a little above are distorted in the negative x- and y-direction, the vorticity gradient has a stabilizing influence and reduces the deformation.

In contrast to this situation, the other ω_z-vorticity maximum high up is not stabilized by the wall and weak against warping. Therefore the longitudinal vorticity of this sheet, which transports slow material to the centerline, will warp the ω_z -concentration which in turn amplifies the ever increasing longitudinal vorticity. When the warping becomes more pronounced a new and more complex flow evolves. The often cited effects of self-induction, stretch and the induction of the images come into play. They altogether contribute to an avalanche of events which disregarding all other respects, exhibits also a great aesthetic appeal. This may be illustrated by a movie.

At this point it may be appropriate to mention shortly another type of three-dimensional instability. We found a wavy motion in spanwise direction nearly independent of z over a large part of the tunnel, when the ribbon amplitude or the ribbon distance from the wall varies linearly with z.

It seems that also the non-uniform spanwise amplitude of the Tollmien wave gives rise to this simpler unstable three-dimensional motion. We got the impression that this motion has also a shingle structure. Its amplification seems to be bound to the Tollmien wave and is much less as with the symmetrical event described above. Nevertheless, this special type of three-dimensional motion may deserve more attention because we have occasionally observed that this swinging motion can also lead to breakdown. Furthermore it is felt that the symmetrical case discussed above may in its early stage be composed by two such opposite motions.

5. CONCLUSIONS

Detailed measurements of the three-dimensional motions upstream of a breakdown region on a flat plate boundary layer suggest that the incipient three-dimensional structure, which follows the purely two-dimensional wave with finite amplitude, contains longitudinal counterrotating vorticity sheets, which are inclined downstream and overlap each other like roof shingles. It is believed that this new model describes the basic configuration, which leads through several intermediate and even more instable states into turbulence.

6. ACKNOWLEDGEMENTS

The author wishes to thank Dipl.Ing. M. Strunz for his continuous help and patient assistance.

7. REFERENCES

/1/ Klebanoff, P.S., K.P.Tidstrom, L.M.Sargent: The three-dimensional nature of boundary instability. J.Fluid Mech.12 (1962) p.1-34

/2/ Wortmann, F.X.: Experimentelle Untersuchungen laminarer Grenzschichten bei instabiler Schichtung. Proc.XI.Int.Congress Appl.Mech. Munich 1964, p.815-825

/3/ Kovasznay, L.S.G., H.Komoda, B.R.Vasudeva: Detailed Flow Field in Transition. Proc.1962 Heat Transf. & Fluid Mech.Inst., p.1-26

/4/ Theodorsen,T.: The structure of turbulence. 50 Jahre Grenzschichtforschung 1955 (Ed.H. Görtler und W.Tollmien) p.55-62, Braunschweig Vieweg u.Sohn

/5/ Hama, F.R., J.Nutant: Detailed Flow-Field Observations in the transition Process in a thick boundary layer. Proc.1963 Heat Transf. and Fluid Mech.Inst., p.77-87

Table I: u'/u_∞ fluctuation at z = 3 and z = -11 cm (in percent)

x_1 cm	z = -3 cm	z = -11 cm
0	0,74	0,74
10	1,3	1,3
20	2,5	2,5
30	3,8	4,0
40	5,5	6,2
50	7,4	9,2
60	9,7	15

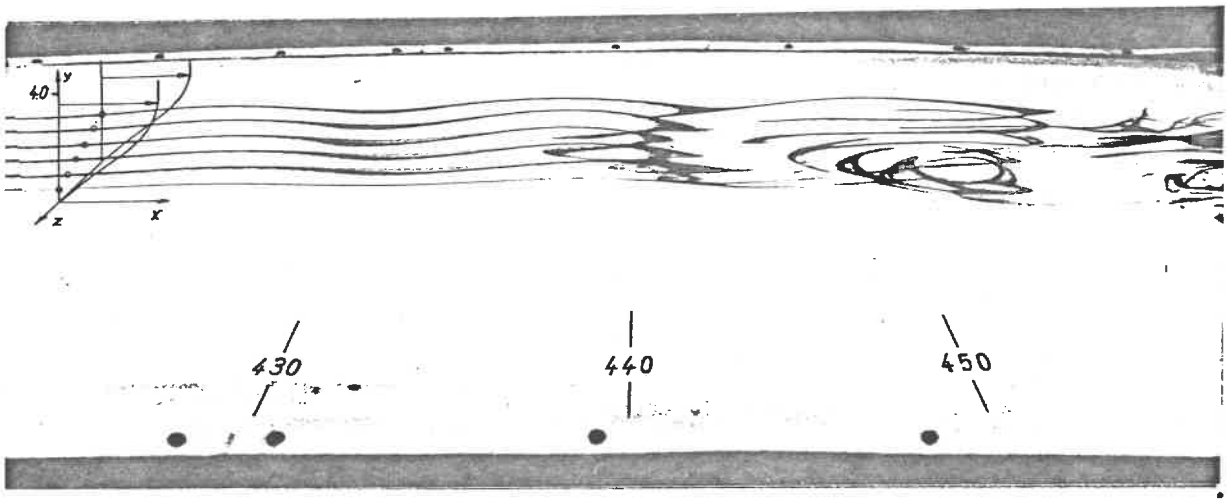

Fig.1: Streaklines in Tollmien-Schlichting waves near breakdown

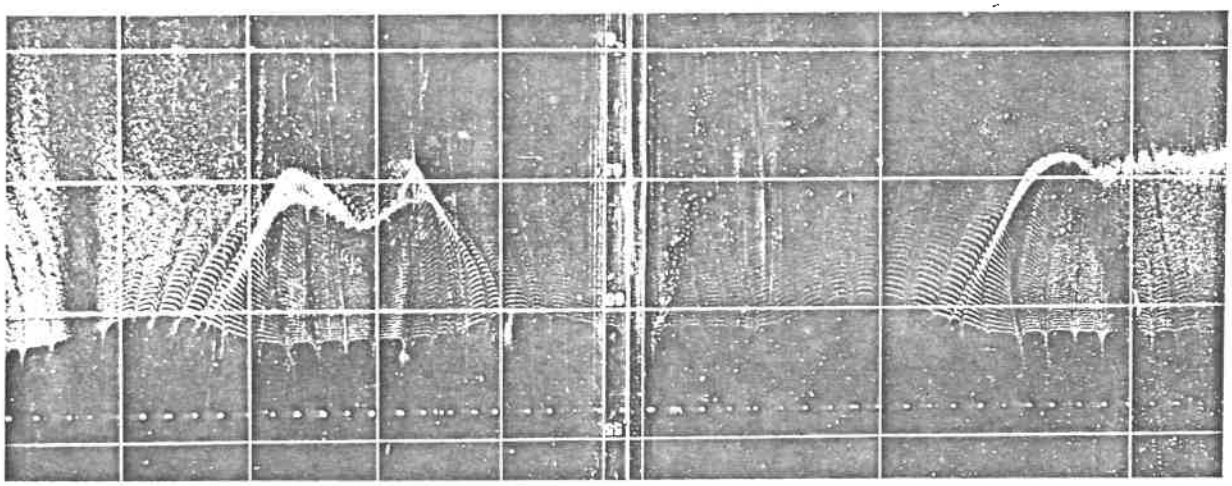

Fig.2: Three-dimensional deformation of timelines of hydrogene bubbles at different spanwise positions. The numbers denote the x -position and the centerline of the tunnel

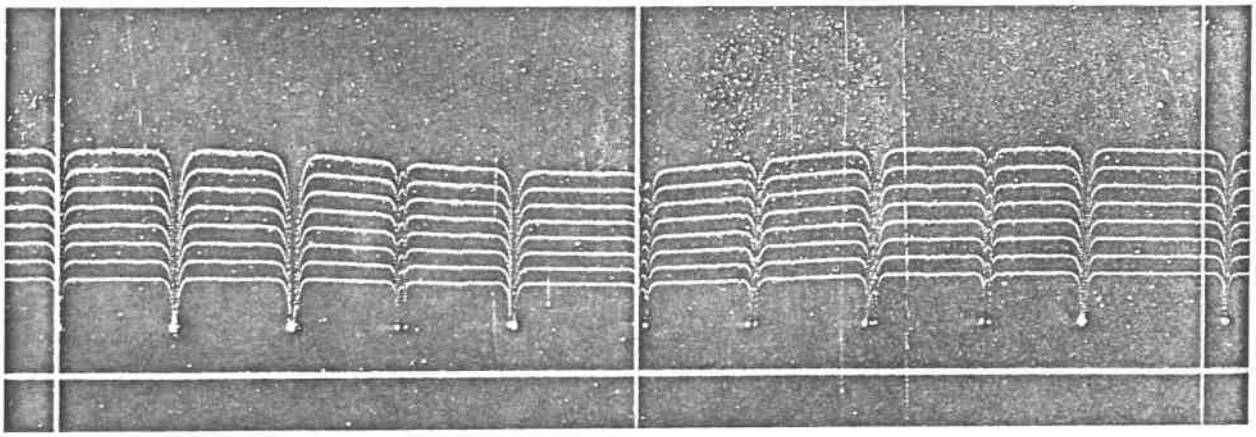

Fig.5: u(z) and w(z) between z = -5 and z = -15 cm for a certain wall distance and phase position

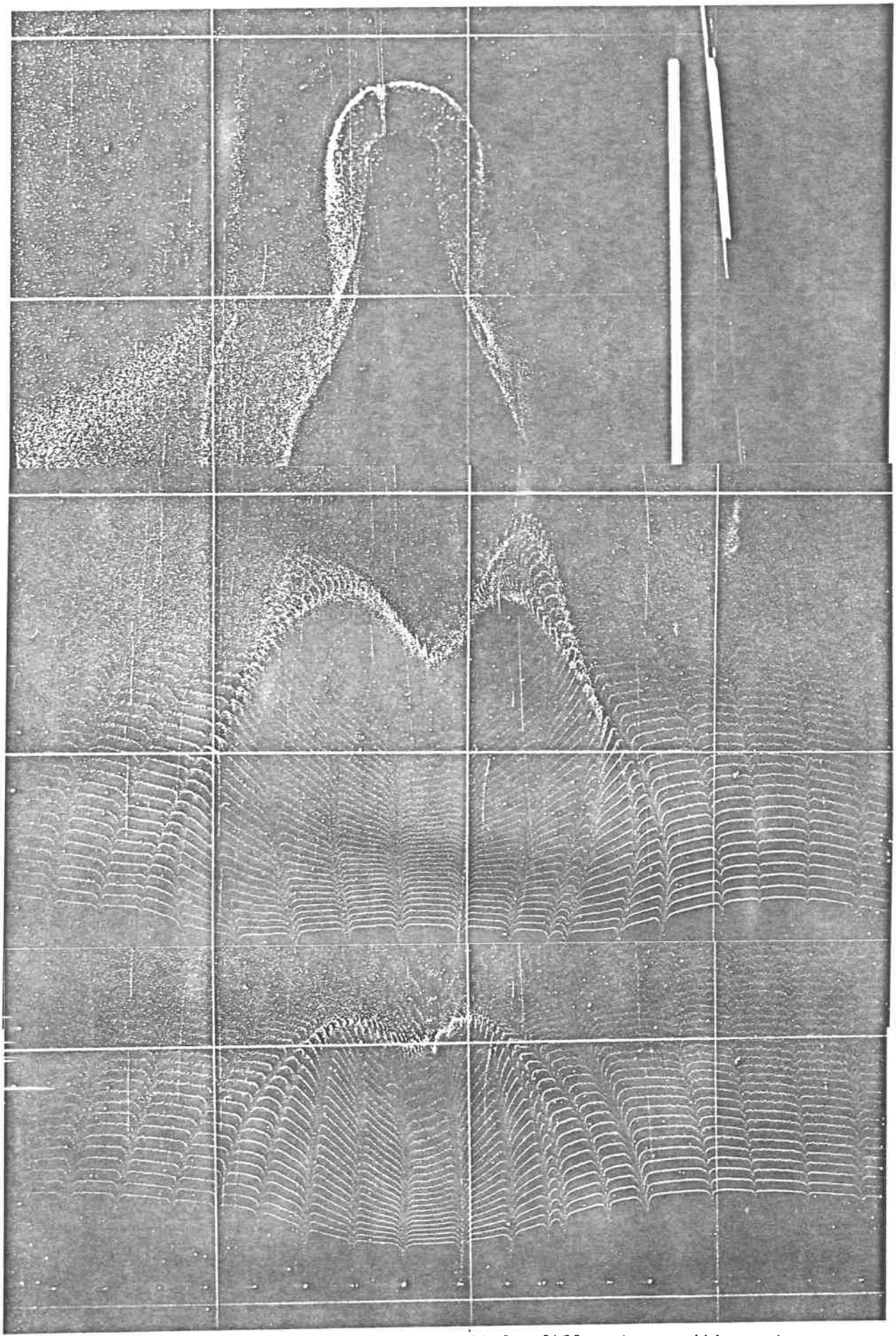

Fig.3: Deformation of timelines around z = -11 cm for different x-positions at x_1 = 55, 60 and 65 cm

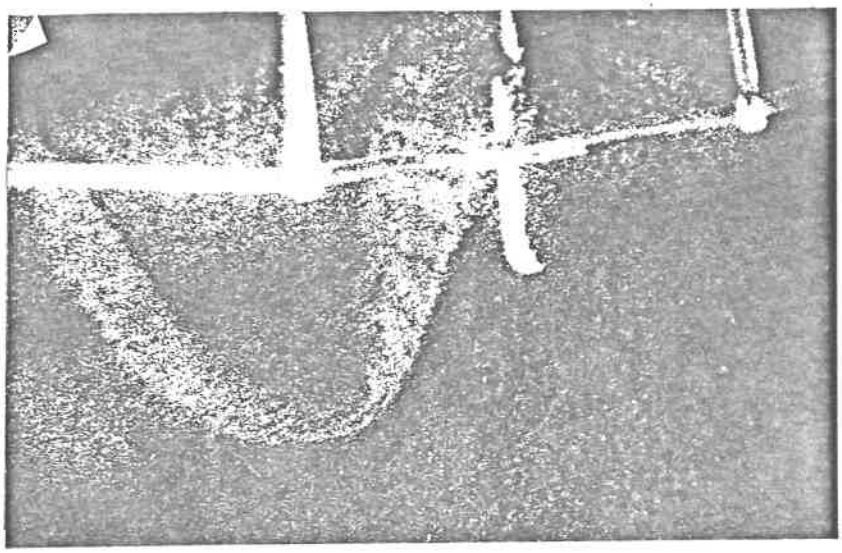

Fig.4:
Vortex loop near the wall.
The bright structure is part of the probe

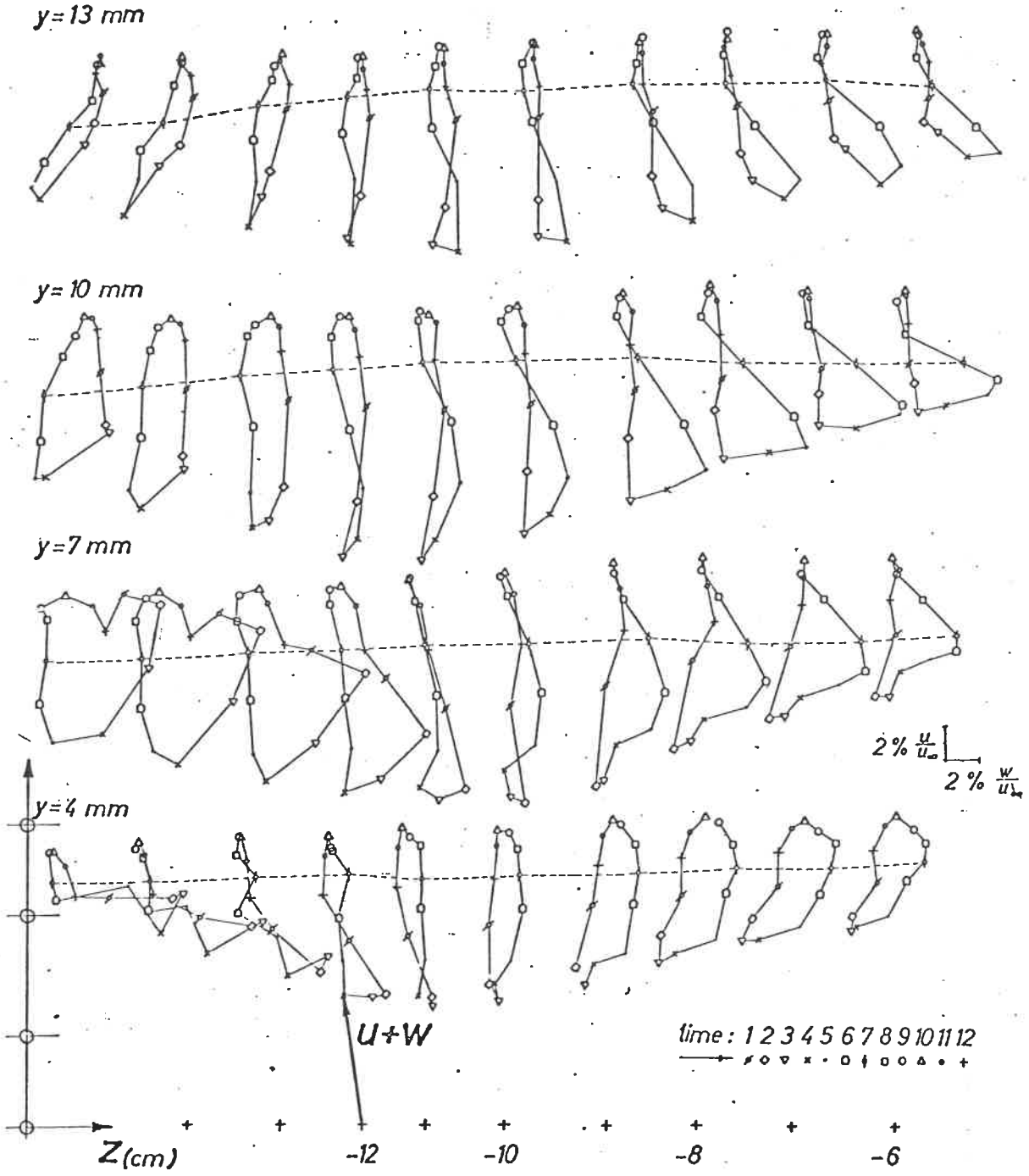

Fig.6: Loops of the velocity vector u + w for one wave period at four different wall-distances for $-16 < z < -5$ cm, $x_1 = 40$ cm

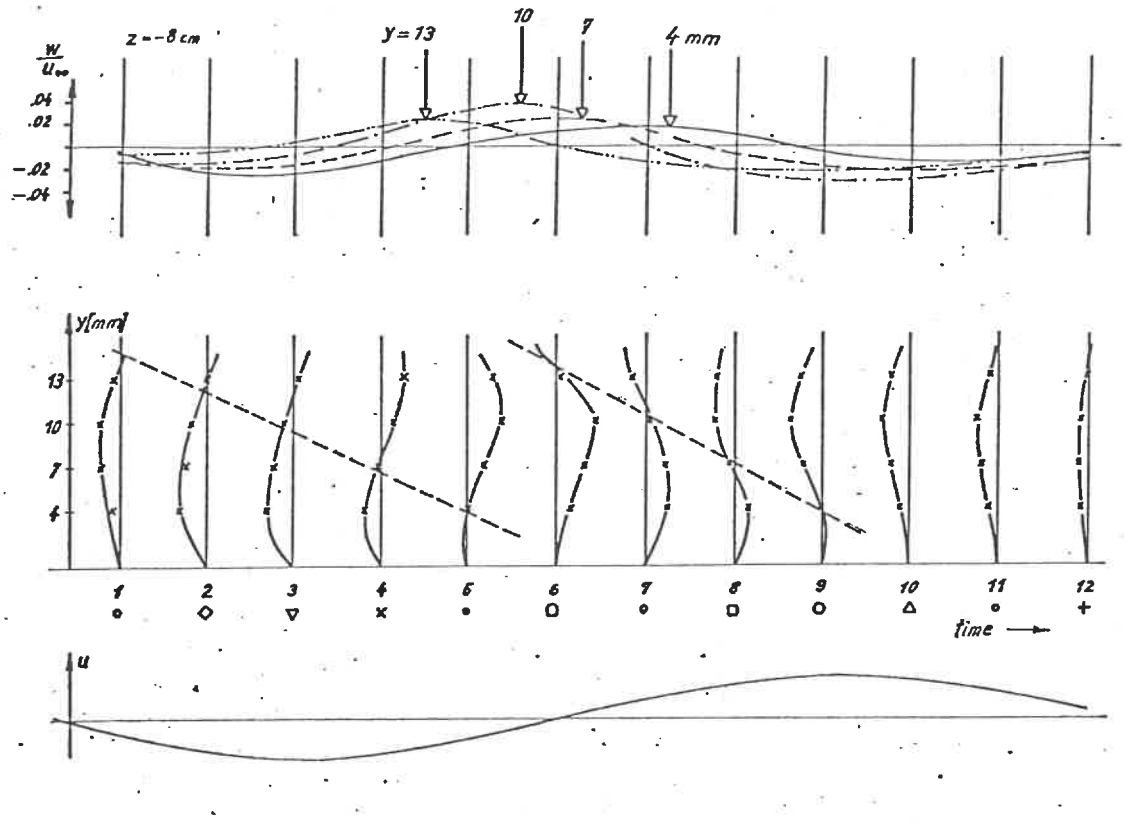

Fig.7: w-component at four heights over one period, taken from Fig.6 for z = -8 cm. In the lower part the nodal points of w(y) are accentuated by dashed lines.

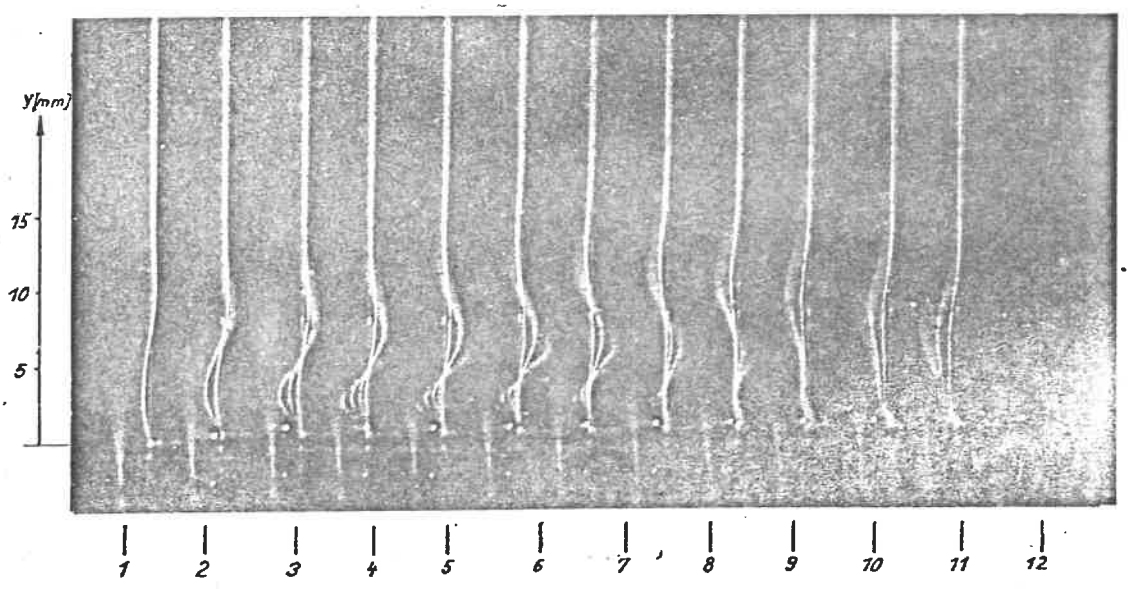

Fig.8: Photographed boundary layer profiles, seen upstream in flow direction at z = -7 cm, x_1 = 40 cm for different phase positions.

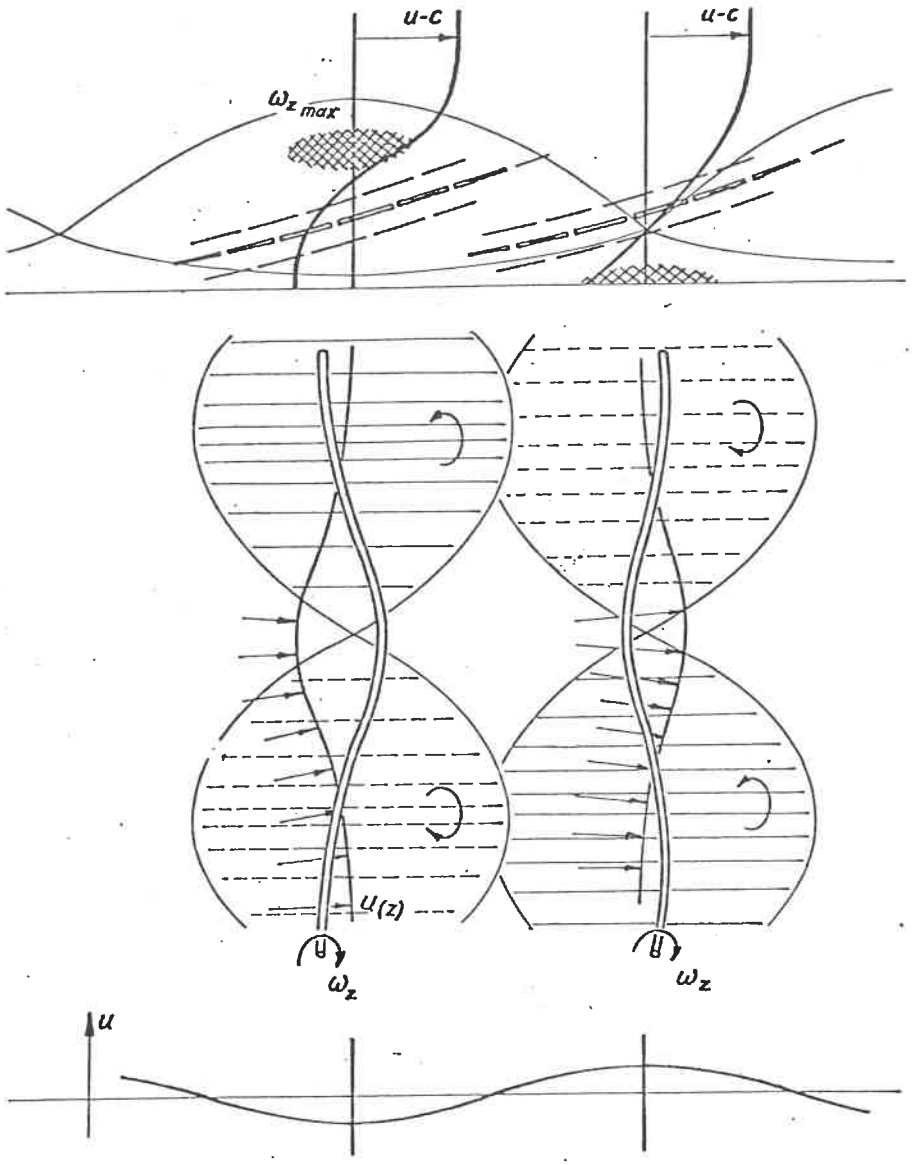

Fig.9: Planform and side view of the $\omega_x+\omega_y$ -vorticity relative to the basic wave and the local ω_z maxima.